SSRG International Journal of Computer Science and Engineering
ISSN: 2348–8387 / https://doi.org/10.14445/23488387/IJCSE-V11I8P107

Volume 11 Issue 8, 50-60, August 2024


*Original Article*

# Developing a Vehicle Plate Recognition System for Degraded Images

Dania Anouwer[1], Nada Jasim Habeeb[2]

*[1,2]Department of Information Technology, Technical College of Management, Baghdad, Iraq.*

*[1]Corresponding Author : dac2011@mtu.edu.iq*

Received: 26 June 2024 Revised: 31 July 2024 Accepted: 21 August 2024 Published: 31 August 2024

***Abstract*** *- The implementation of a vehicle plate recognition system holds significant importance within the domain of vehicle monitoring, particularly in the context of traffic management applications. However, this system is often subjected to adverse weather conditions, including fog, dust, and rain, as well as varying lighting scenarios, all of which may lead to high levels of noise in the captured images, consequently impeding the accurate identification of vehicle plate numbers. A recent study has introduced a method aimed at enhancing the recognition of vehicle plate numbers by employing the use of three denoising filters to effectively improve image quality, with a focus on identifying the optimal filter. Though these filters have proven successful in noise reduction, they have also been noted to introduce blurring in the resultant images due to the mathematical operations involved, causing a reduction in high-frequency values within the images. To address this challenge, a deblurring Wiener approach has been integrated. As a result of these enhancements, the automatic recognition method proposed in this study has demonstrated a marked improvement in the identification of vehicle plate numbers and letters, outperforming systems designed for the recognition of distorted plates, which may encounter distortion rates of up to 70%.*

***Keywords*** *- License plate recognition, De-noising filters, Deblurring filter, Wiener filter, Degraded image.*

## 1. Introduction

Automated License Plate Recognition (ALPR), also known as vehicle license plate recognition, is an optical character recognition technology utilized to scan vehicle license plates and convert them into computer-readable data. This process involves the use of images captured by video cameras to analyze the characters on the license plates. However, environmental factors such as bad weather conditions, damage during transmission over the Internet, or noise originating from a noisy sensor can cause distortion or noise, making it challenging to accurately detect and recognize the numbers and letters on the plate. This noise typically manifests as isolated pixel changes that are visually distinct from their neighboring pixels. To address this issue, image processing techniques are employed to retrieve license plate information from an image or video frame. The extracted data finds applications in various fields, including electronic payment gateways, parking fee payment systems, road monitoring systems, and traffic management systems [1, 2]. Various methods have been developed in this field that perform well under conditions like noise, fog, and low light. Many studies have recently offered ways to recognize vehicle license plates in degraded images. Rai, V., and Kamthania, D. (2024) [3] introduced a system designed to identify vehicle license plates and capture their images. The main objective of this system is to facilitate precise extraction of license plate information, prioritizing accuracy, automation, and versatility. Moreover, it offers a robust solution for comprehensive traffic monitoring and enforcement by integrating vehicle speed calculations. Tiwari, A. et al. (2023) [4] proposed an Automatic Vehicle Number Plate Recognition system leveraging the capabilities of YOLOv8 (You Only Look Once) and Convolutional Neural Networks (CNN). The primary aim of this system is to expedite the accurate extraction of license plate details, focusing on precision, automation, and adaptability. Pujar, A. M. and Kulkarni, P. B. (2023) [5] aimed to develop a dependable automatic vehicle recognition system utilizing vehicle number plates. For number plate detection, an infrared (IR) sensor is employed to capture clear images from the camera. This technology finds application in various areas, such as traffic control, automatic road tax collection in toll areas, and parking systems in congested areas. Given the remarkable performance of deep networks compared to other machine learning techniques, the focus is primarily on license plate recognition methods based on neural networks. Alam, N. A et al. (2021) [6] highlighted the pivotal role of intelligent systems in traffic control through vehicle number plate detection. In recent years, a vehicle number plate detection and recognition system has been developed using a Convolutional Neural Network (CNN) and deep learning techniques. Kim, Tae-Gu et al. (2021) [7] recommended a technique that employs a deep learning model trained on an extensive database to address challenges encountered in recognizing vehicle license plates via closed-circuit video (CCTV). Pustokhina, I. V. et al. (2020) [8] introduced the OKM-CNN model, a powerful deep learning-based Vehicle License Plate Recognition (VLPR) model that utilizes optimum K-means (OKM) clustering-based segmentation and Convolutional Neural Network (CNN) based recognition. Maier, A. et al. (2022) [9] The study aimed to utilize machine learning techniques to interpret license plates from low-quality images accurately. In this research, a Bayesian Neural Network was introduced to encompass an inherent reliability measure for the classifier.

Furthermore, the proposal suggests integrating multiple estimations with an entropy weight to enhance the reliability of the system further. Kaiser, P. et al. (2021) [10] The generally low image quality and strong compression often make it difficult to read license plates. This paper aims to address this issue by investigating the impact of JPEG compression on license plate recognition from highly degraded images. The study demonstrates the effectiveness of CNN on a real-world dataset of Czech license plates. The prior research on license plate recognition has demonstrated that the proposed systems in most of these studies perform effectively under low levels of noise, blur, or other forms of damage. However, their efficacy diminishes when handling images of damaged license plates that have lost significant information and details. In response, the paper presents a system designed to automatically discern the contents of license plates that have been compromised under specific conditions. This is achieved through the utilization of robust filters to address issues such as high noise and blur. The ultimate aim is to enhance the test images before subjecting them to the discernment process. The paper is organized as follows: Section 2 presents the background and the theoretical topics used in this work. The suggested plate recognition method is based on a de-noising filter and deblurring filter. In Section 3, the proposed work's features, components, and system design are explained. In section 4, the experimental results are presented. Finally, Section 5 presents the conclusion.

## 2. Background

In this section, a brief overview of the methods used in the proposed license plate recognition system is provided.

### *2.1. License Plate Recognition*

The process of recognizing vehicles through license plate identification involves several key steps, including image preprocessing, character segmentation, and advanced recognition technology. Preprocessing is a vital stage as it enhances the quality and information extracted from the input image. Techniques such as image resizing, enhancement, noise reduction, binarization, and morphological operations are commonly employed to ensure consistent results, reduce computational complexity, minimize noise, simplify subsequent processing, and enhance the accuracy and efficiency of character recognition and pattern matching [11]. Character segmentation is crucial in license plate recognition as it involves isolating individual characters within the license plate image. This step is essential for gathering alphanumeric data that can be further processed for character recognition extraction. Connected component analysis, contour detection, projected contour-based methods, and machine learning approaches are commonly used techniques for effective character differentiation and extraction, addressing challenges related to font, size, spacing, and potential noise. Character segmentation is imperative for achieving precise and dependable license plate recognition [12]. In license plate character recognition, the template matching approach is utilized to detect all segmented characters. It involves comparing a character's template image with various areas of the number plate image to identify matches [13].

### *2.2. Denoising Filter*

One of the recognized forms of interference is impulse noise, which manifests as speckles of bright and dark pixels, also referred to as salt-and-pepper noise. This type of noise can introduce random distortions to an image, potentially causing data dropouts and leading to image corruption during data transmission. The characteristics of this noise can be formally described as [14].

$$\boldsymbol{P(z)} = \begin{cases} \boldsymbol{P_a} & \boldsymbol{z = a} \\ \boldsymbol{P_b} & \boldsymbol{z = b} \\ \boldsymbol{0} & \boldsymbol{otherwise} \end{cases}$$

, for an 8-bit image, the pixel values are represented as a = 0 for black and b = 255 for white.

Denoising holds great significance in the field of image processing as it contributes to enhancing content quality and preserving image integrity. The presence of noise can significantly reduce clarity and disrupt processes such as semantic segmentation and classification, underscoring the necessity for dependable approaches to tackle this challenge [15].

### *2.3. Deblurring Filter using Wiener Filter*

Image deblurring is a crucial technique employed to rectify blurriness and improve the sharpness of a distorted image. Blurring can stem from various factors such as camera shake, motion blur, or misfocused capture. The primary goal of image deblurring is to reinstate the original details and elevate the visual quality of the image. The Wiener filter is a prominently utilized method for image deblurring, with its focus on minimizing the mean square error between the original image and the blurred one [16]. Evaluation Metrics:

1) The Mean Squared Error (MSE) is utilized to compute the average of error squares. Given two images represented by g (n, m) and ĝ (n, m), the MSE for an image is defined as follows:

$$\boldsymbol{MSE = \frac{1}{mn} \sum_m \sum_n (x_{mn} - y_{mn})^2} \tag{1}$$

In the context where "m" denotes the number of rows, "n" signifies the number of columns, and "$\boldsymbol{x_{mn}}$" and "$\boldsymbol{y_{mn}}$" denote the value of pixel [17].

2) the peak signal-to-noise ratio (PSNR) serves as a metric to quantify a signal's highest strength relative to the impact of distorting noise on the fidelity of representation. The PSNR is formally defined as stated in reference [18].

$$\boldsymbol{PSNR(x,y)} = \frac{\mathbf{10\log_{10}(max(max(}x\mathbf{),max(}y\mathbf{)))^2}}{|x-y|^2} \tag{2}$$

3) The Structural Similarity Index Metric (SSIM) assesses the similarity between the resulting image and the initial input picture. When the index surpasses 0.95, it indicates effective image reconstruction. This metric considers three primary aspects: contrast distortion, loss of correlation, and luminance distortion. The SSIM is mathematically represented as [19].

$$SSIM = \frac{(2_{\mu x \mu y}+C_1)(2_{\sigma xy}+C_2)}{(\mu_x^2+\mu_y^2+C_1)(\sigma_x^2+\sigma_y^2+C_2)} \tag{3}$$

$$Here, \mu_x = \sum_{i=1}^{N} \omega_i x_i \tag{4}$$

$$With, \sigma_x = \sqrt{\sum_{i=1}^{N} \omega_i (x_i - y_i)^2} \tag{5}$$

$$And, \sigma_{xy} = \sum_{i=1}^{N} \omega_i (\, x_i - \mu_x)(y_i - \mu_y) \tag{6}$$

In the above formula, N = 121 represents the number of pixels in the window, $C_1 = (0.01 \times \mathrm{L})^2$,$C_2$ $(0.03 \times \mathrm{L})^2$, L = 255 represents the dynamic range, $x_i$ and $y_i$ are pixel values and $\omega_i$ is a value from the 11×11 matrix of samples from the 2D Gaussian with σ = 1.5.

### *2.4. Sharpening or Focus Operators*

Focus measure operators are utilized to assess the sharpness and focus of an image or image pixel. Each measure is thoroughly described as follows:1) Image contrast (CONT) [20].

$$C(x,y) = \sum_{i=x-1}^{x+1} \sum_{j=y-1}^{y+1} |\, f(x,y) - f(i,j)| \tag{7}$$

2- Gaussian derivative (GDER) [21]

A focus measure for autofocus in microscopy based on the first-order Gaussian derivative

$$FM = \sum_{(x,y)} (f * \Gamma_x)^2 (f * \Gamma_y)^2 \tag{8}$$

Where Γ_x and Γ_y are the x and y partial derivatives of the Gaussian function

$\Gamma(\mathrm{x,y},\sigma)$, respectively

$$\Gamma(\mathrm{x,y},\sigma) = \frac{1}{2\pi\sigma^2} \exp\left(-\frac{x^2+y^2}{2\sigma^2}\right) \tag{9}$$

3- Gradient energy (GRAE) [22]

$$FM_{x,y=} \sum_{(i,j)\in\Omega(x,y)} (f_x(i,j)^2 + f_y(i,j)^2) \tag{10}$$

3- Histogram entropy (HISTE) [23]

The histogram entropy operator is defined as

$$FM = -\sum_{k=1}^{L} P_k \log(P_k) \tag{11}$$

Where $P_k$ is the relative frequency of the k-th gray-level.

4- Spatial frequency (SFRQ) [24]

$$FM_{x,y} = \sqrt{\sum_{(i,j)\in\Omega(x,y)} f_x(i,j)^2 + \sum_{(i,j)\in\Omega(x,y)} f_y(i,j)^2} \tag{12}$$

Where $f_x$ and $f_y$ denote the first derivatives of a frame in the X and Y direction, respectively.

## 3. Components of License Plate Recognition System

Image processing involves several critical preprocessing steps that are essential for tasks such as license plate identification. Normalization is a crucial step in preparing images uniformly to enhance the performance and accuracy of the recognition system [25]. Converting images to binary format (black and white) is a common preprocessing step in license plate recognition, simplifying the image to facilitate character segmentation and identification on the license plate [26]. Dilation, a morphological procedure used in image processing, is particularly beneficial in license plate identification systems. It extends the white regions in a binary picture, aiding in linking neighboring objects and filling minor gaps or holes in the text or license plate [27]. In the process of number plate detection, several phases are involved, encompassing image capture, preprocessing, number plate localization, character segmentation, and character recognition [28,29]. When addressing character segmentation for license plates, each individual character within the identified license plate region is individually processed for recognition. This technique involves analyzing the entire binarized image and identifying all relevant components within the image [30]. Subsequently, in the final stage, the template matching approach is applied to identify all segmented characters. Template matching, a digital image processing technique, entails comparing the small components of an image to a predefined template [12].

## 4. Proposed Number Plate Recognition System

The conventional methods for number plate recognition often struggle to differentiate between digits in images affected by noise and blur. Therefore, it is imperative to develop a system that can accurately identify all types of images, irrespective of their clarity or damage, even when the damage significantly obscures the information. The proposed system's flow diagram is depicted in Figure 1.

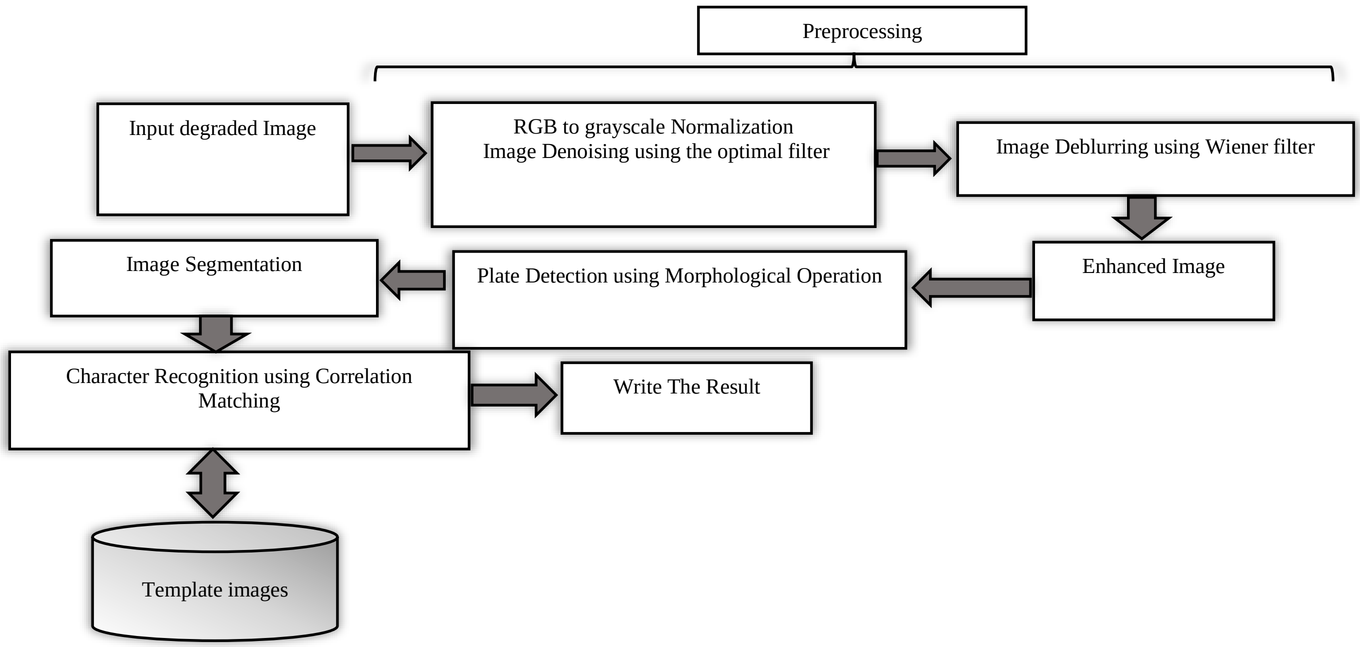


**Fig. 1 Proposed number plate recognition system for degraded images**

The document outlines the proposed process for number plate recognition in the following steps:
Step 1: The initial step involves a preprocessing process for the input image. This includes converting the image to grayscale. Each pixel in the color image, which consists of red, green, and blue (RGB) values, is transformed into a single gray value using a mathematical formula to represent the intensity of the gray color.

$$Gray_{Img} = RGB\_to\_Gray\ (Img)$$

To enhance precision and accelerate the system's performance, it is essential to convert the gray image into a double format. This involves the conversion of the pixel values, originally 8 bits ranging from 0 to 255, to a double type ranging from 0 to 1, enabling accurate calculations and system optimization.

$$G\_Image = double\ (Gray_{Img})$$

Applying denoising filters to the degraded gray image (G _ Image) involved the use of three different filters to remove noise: Nearest Value Based Mean Filter (NVBMF), Noise Accumulation and Harmonic Analysis Techniques (NAHAT), and Different Adaptive Modified Riesz Mean Filter (DAMRFM). These filters are known for their high noise removal capability, achieving density levels of up to 70%. Comprehensive details about these filters can be found in [31, 32,33], respectively. After the application of filters, it is essential to calculate various quality measures to assess the impact on the images. These measures, including Peak Signal-to-Noise Ratio (PSNR), Mean Square Error (MSE), and Structural Similarity Index Measure (SSIM), help objectively evaluate the image quality. PSNR evaluates the signal-to-noise ratio of the original image, with higher values indicating better image quality. MSE measures the average square difference between pixel values, where a smaller value signifies better image quality. SSIM assesses the structural similarity between the original and the resulting images, with higher values indicating superior image quality. In the second step of the process, proceed to select the optimal denoising filter based on the previously computed quality measures. The search for the best value involves evaluating three different filters: a) PSNR_max - the maximum value of the PSNR index, b) MSE_min - the minimum value of the MSE index, and c) SSIM_max - the maximum value of the SSIM index. Moving on to the third step, despite the enhancements made in the previous step, the image still exhibits blurriness. Consequently, the Wiener filter, recognized as one of the most effective options for reducing blurriness in images, can be applied to obtain the final enhanced image with sharper clarity. In step 4, the sharpening metrics are calculated by evaluating various factors such as contrast ratio (CONT), slope absolute error rate (GRAE), histogram energy efficiency (HISTE), spatial frequency of signals (SFRQ), and image entropy. These metrics are instrumental in determining the quality of sharpening achieved on the filtered image. Moving on to step 5, the final enhanced image is utilized as the input for the Number Plate Recognition system. Upon the splitting of the extracted license plate into individual character images, different methods can be employed to identify the characters within each image. Specifically, for this system, template matching was carried out using a correlation function to compare the match between the character segment and the templates stored in the database. The recognized character was the one that yielded the highest match.

### *4.1. Experimental Results*

#### *4.1.1. Results of Input Images with different Noise Levels*

The proposed algorithm's performance was evaluated using a variety of vehicle plate images sourced from different websites. For the presentation of results, only two images (Img.1, Img.2,….Img5) were chosen. The results in Figure 2 display the outcomes of the noisy images, encompassing noise density levels from 10% to 70%.

Additionally, Table 1 provides an overview of the quality metric values for the noisy images. Based on Figure 2 and Table 1, it is evident that as the noise density increases, there is a noticeable decrease in image quality. This results in the distortion of information within the image, ultimately posing challenges for traditional number plate recognition systems when it comes to recognizing the numbers in the image.

**Table 1. Quality metric values for noisy images with different noise levels**

| Data Set | Metrics | 10 % Noisy Density | 30 % Noisy Density | 50 % Noisy Density | 70 % Noisy Density |
|---|---|---|---|---|---|
| **Img.1** | PSNR | 14.5158 | 9.7804 | 7.5558 | 6.0940 |
| | MSE | 2.2988e+03 | 6.8397e+03 | 1.1416e+04 | 1.5984e+04 |
| | SSIM | 0.2106 | 0.0827 | 0.0439 | 0.0227 |
| **Img.2** | PSNR | 14.4597 | 9.7303 | 7.5078 | 6.0833 |
| | MSE | 2.3287e+03 | 6.9191e+03 | 1.1543e+04 | 1.6023e+04 |
| | SSIM | 0.2090 | 0.0804 | 0.0426 | 0.0231 |
| **Img.3** | PSNR | 14.1150 | 9.2718 | 7.0440 | 5.5953 |
| | MSE | 2.5210e+03 | 7.6896e+03 | 1.2843e+04 | 1.7929e+04 |
| | SSIM | 0.3071 | 0.1440 | 0.0798 | 0.0426 |
| **Img.4** | PSNR | 13.7707 | 10.7347 | 6.7469 | 5.3101 |
| | MSE | 2.7291e+03 | 5.4904e+03 | 1.3753e+04 | 1.9145e+04 |
| | SSIM | 0.3543 | 0.2359 | 0.1041 | 0.0542 |
| **Img.5** | PSNR | 14.4513 | 9.7958 | 7.5795 | 6.0340 |
| | MSE | 2.3332e+03 | 6.8155e+03 | 1.1353e+04 | 1.6206e+04 |
| | SSIM | 0.2105 | 0.0826 | 0.0459 | 0.0212 |

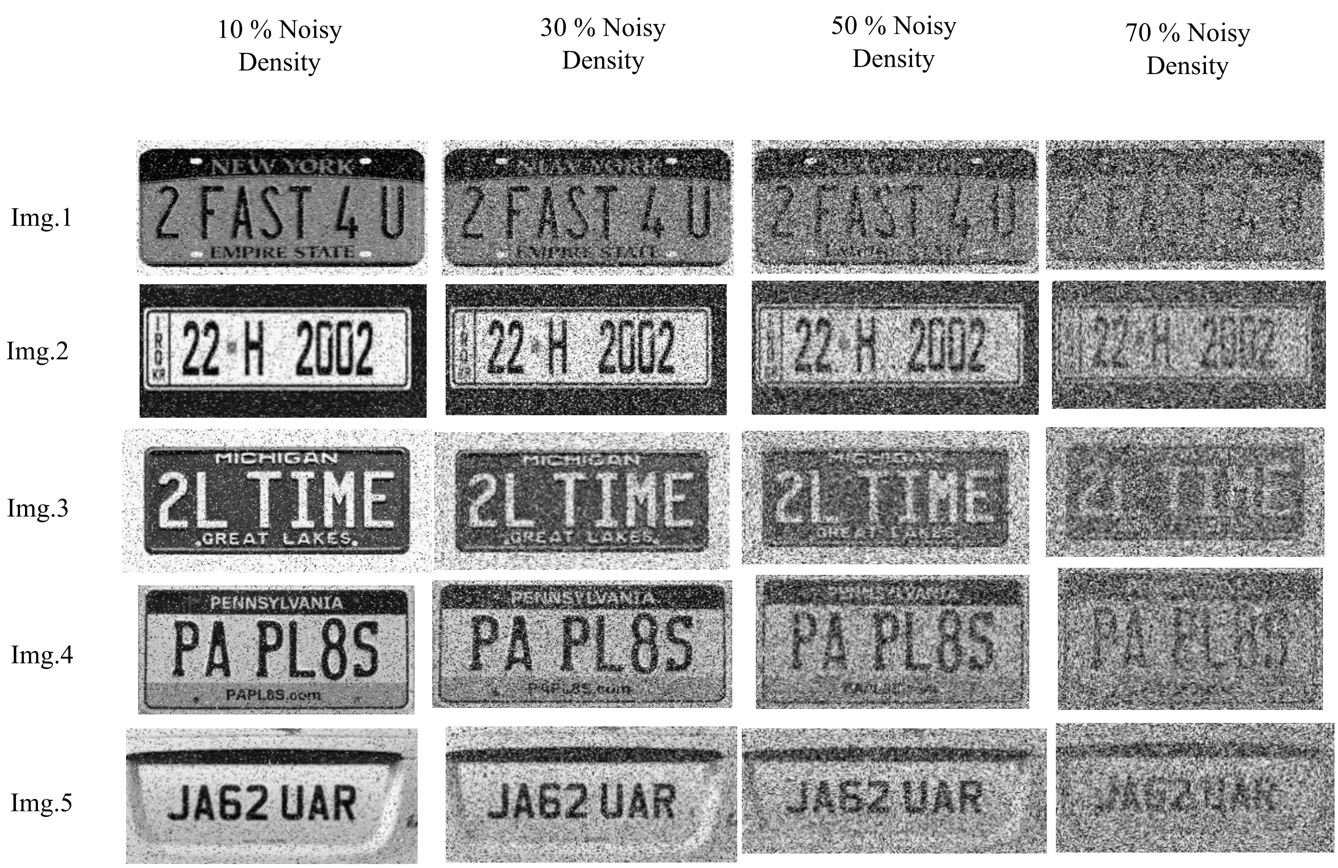


**Fig. 2 Shows a set of images with different levels of noise**

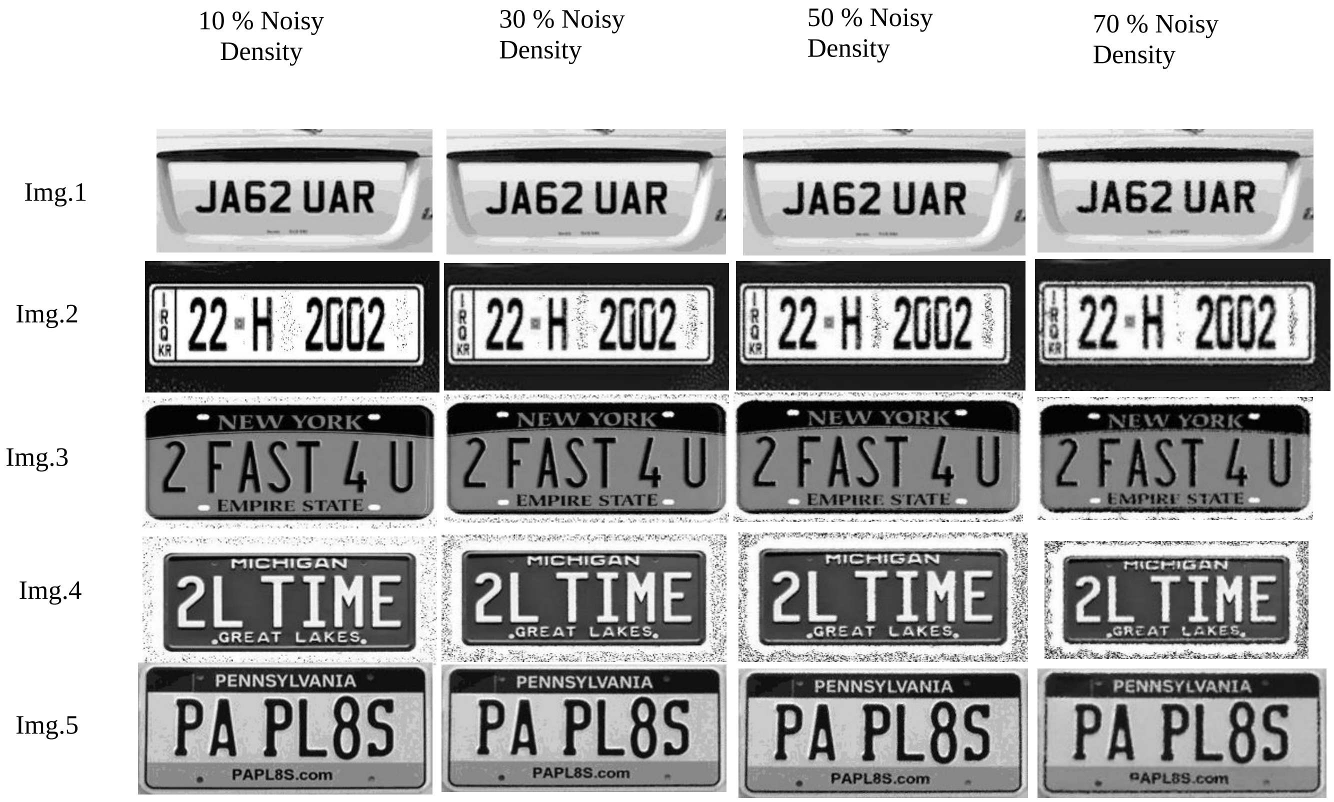


**Fig. 3 Shows a set of images after removing different percentages of noise using the (DAMRMF) filter**

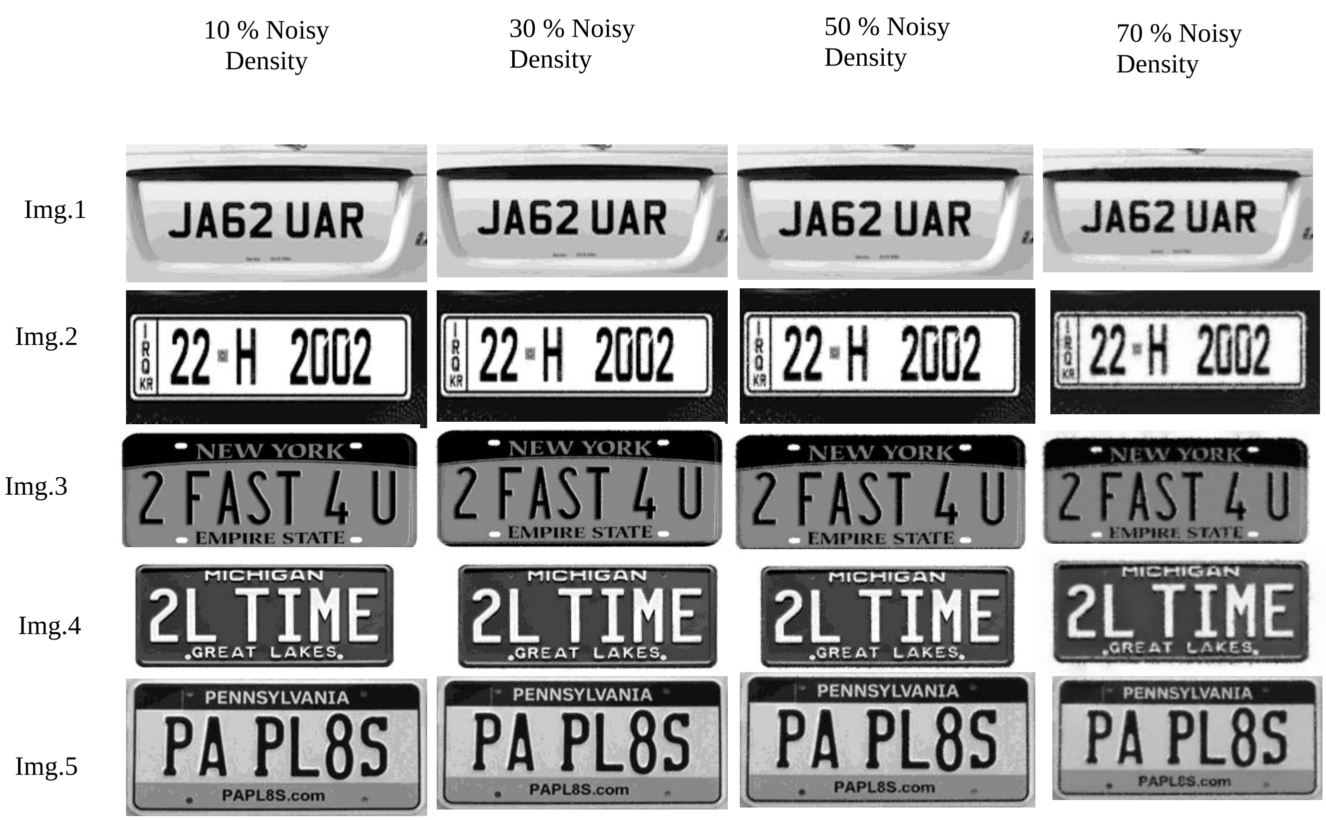


**Fig. 4 Shows a set of images after removing different percentages of noise using the (NAHAT) filter.**

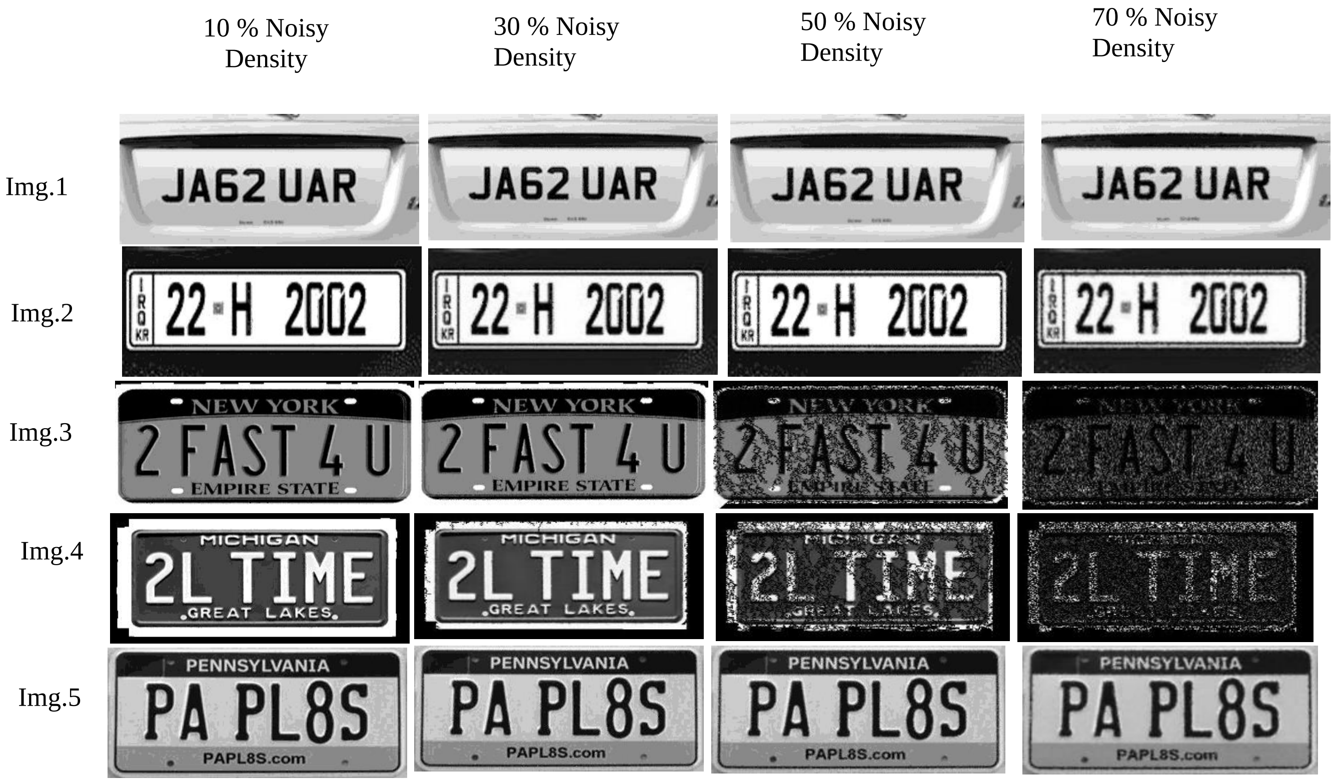


**Fig. 5 Shows a set of images after removing different percentages of noise using the (NVBMF) filter**

*4.1.2. Results of denoising images at different levels*

Figures 3, 4, and 5 show the visual results of removing noise according to the different levels from 10% to 70% using DAMRMF, NAHAT, and NVBMF, respectively. From the above numbers and table, the NAHAT noise removal filter outperforms other filters, and therefore, it is considered the best filter because it has the lowest MSE.

*4.1.3. Evaluate the results of the image deblurring filter*

In Table 3, the Wiener filter stands out with the highest values and best results, making it the optimal choice for dehazing. This filter achieves a fine balance between inverse filtering and noise smoothing, effectively eliminating noise while reversing haze. The Wiener filter's superiority lies in its ability to minimize mean square error, thus reducing errors in both inverse filtering and noise smoothing. It essentially serves as a linear approximation of the original image.

*4.1.4. Result of Recognition*

The final step in the proposed system involves the recognition of the number in the license plate image. This process can be outlined as follows:

*Image Reading*

The system reads the image of the degraded license plate.

*Preprocessing*

This crucial step entails enhancing the image quality by applying optimal filters to eliminate noise and blur.

*Plate Detection*

In this stage, the system identifies and extracts the license plate area from the pre-processed image using morphological operations such as stretching and erosion.

*Image Binarization*

This step converts the grayscale image into a binary image. Generally, image binarization leverages the grayscale pixel information to compute a threshold value, which is subsequently used to classify image pixels as background or foreground.

*Character Segmentation*

Finally, the characters on the license plate are segmented individually to prepare them for recognition.

*Character Recognition*

After segmenting each character, recognition is achieved through a matching process with a character database consisting of pre-defined fonts and styles. These templates serve as references for character recognition, facilitating efficient comparison and matching during the recognition phase.

*Character Recognition (Matching and Verification)*

This stage involves comparing the extracted character features with a template database based on pre-defined fonts and styles.

Using the matching Link correlation function, match scores are assigned to potential matches, and a verification process is employed to determine the most accurate definition of personalities.

*Visualizing the Matching Result*

True Positive (TP) denotes cases where the system accurately predicts the positive class. Conversely, a False Positive (FP) occurs when the system mistakenly predicts the positive class while the actual class is negative, as illustrated in Tables 8 and 9.

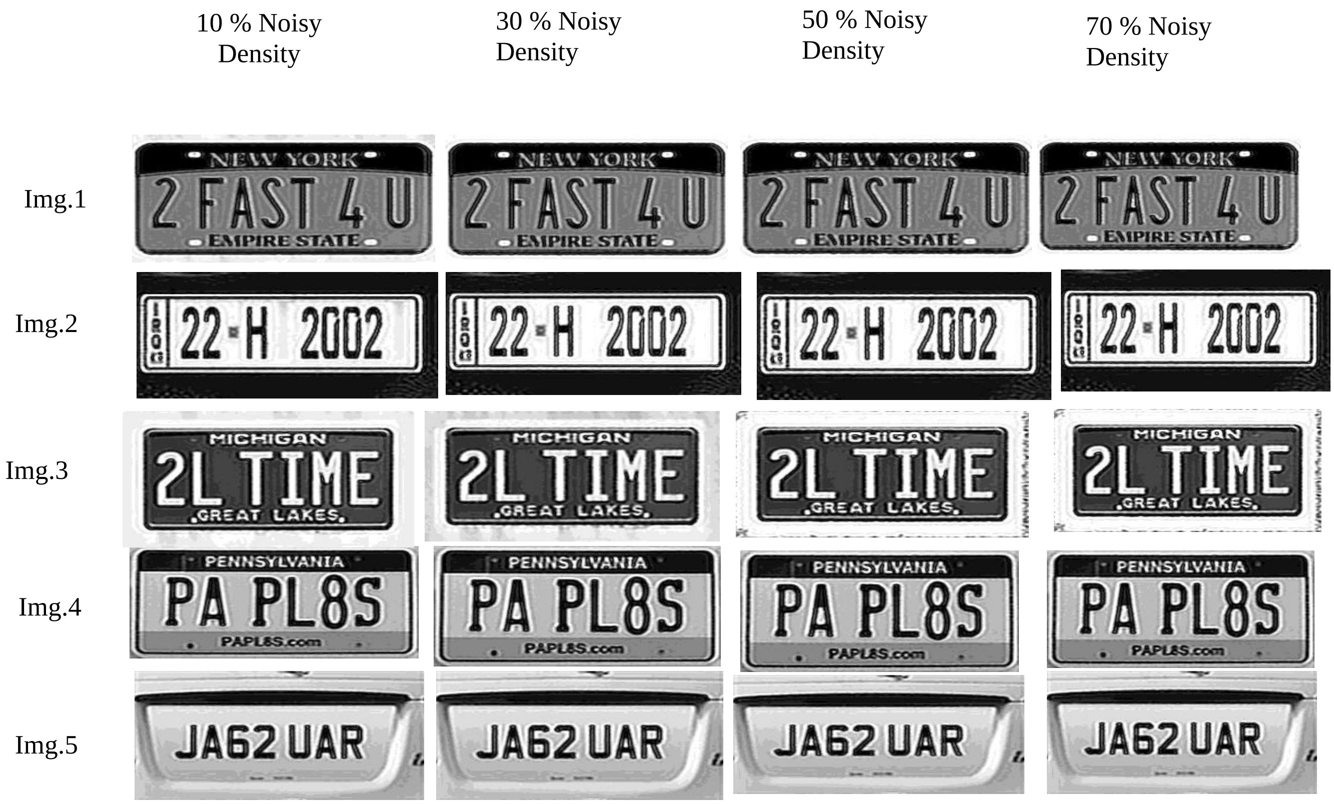


**Fig. 6 Shows the results of images enhanced with the Wiener filter**

**Table. 2 Quality metric values for denoising images with different denoising levels**

| Data Set | Filter Metrics | DAMRmF | NAHAT | NVBMF |
|---|---|---|---|---|
| **Img.1** | PSNR | 38.9855 | 41.2763 | 40.2100 |
| | MSE | 8.2135 | 4.8467 | 6.1955 |
| | SSIM | 0.9948 | 0.9964 | 0.9962 |
| **Img.2** | PSNR | 24.6742 | 32.0609 | 30.8912 |
| | MSE | 221.6444 | 40.4566 | 52.9618 |
| | SSIM | 0.9156 | 0.9818 | 0.9807 |
| **Img.3** | PSNR | 23.6147 | 32.7570 | 17.1520 |
| | MSE | 282.8870 | 34.4650 | 1.2528e+03 |
| | SSIM | 0.9070 | 0.9878 | 0.9482 |
| **Img.4** | PSNR | 19.3002 | 34.0990 | 7.8785 |
| | MSE | 763.9470 | 25.3034 | 1.0598e+04 |
| | SSIM | 0.7568 | 0.9917 | 0.7721 |
| **Img.5** | PSNR | 40.3849 | 42.1328 | 41.4143 |
| | MSE | 5.9510 | 3.9792 | 4.6951 |
| | SSIM | 0.9963 | 0.9974 | 0.9972 |

**Table 3. Shows the results of images enhanced with the Wiener filter**

| Data Set | Noise Level/ Metrics | 10 % Noisy Density | 30 % Noisy Density | 50 % Noisy Density | 70 % Noisy Density |
|---|---|---|---|---|---|
| **Img.1** | CONT | 41.4704 | 42.1472 | 41.3797 | 42.8484 |
| | GRAE | 49.1374 | 49.8165 | 49.4052 | 50.2494 |
| | HISE | 3.7626 | 3.9406 | 3.7629 | 4.0456 |
| | SFRQ | 4.0290 | 4.0624 | 4.0525 | 4.0671 |
| | Image_ entropy | 7.2612 | 7.2716 | 7.2638 | 7.2808 |
| **Img.2** | CONT | 73.0303 | 77.9713 | 76.5941 | 79.4246 |
| | GRAE | 61.0063 | 61.5838 | 63.2753 | 61.3173 |
| | HISE | 7.9265 | 9.9663 | 9.4799 | 10.3741 |
| | SFRQ | 4.7891 | 4.7483 | 4.8713 | 4.6977 |
| | Image_ entropy | 6.7657 | 6.7511 | 6.7550 | 6.7550 |
| **Img.3** | CONT | 66.2852 | 68.4689 | 67.1897 | 70.1350 |
| | GRAE | 73.6783 | 75.3540 | 75.9904 | 75.1722 |
| | HISE | 7.2559 | 7.7551 | 7.4954 | 8.0433 |
| | SFRQ | 5.6448 | 5.6945 | 5.7533 | 5.6541 |
| | Image_ entropy | 7.4882 | 7.3966 | 7.3802 | 7.3979 |
| **Img.4** | CONT | 65.2665 | 78.1037 | 71.6418 | 69.1992 |
| | GRAE | 64.1989 | 81.7322 | 72.8593 | 67.3592 |
| | HISE | 5.3530 | 6.2692 | 6.1863 | 6.0126 |
| | SFRQ | 4.9624 | 6.1375 | 5.5101 | 5.1099 |
| | Image_ entropy | 7.2112 | 7.6680 | 7.1841 | 7.0382 |
| **Img.5** | CONT | 77.3557 | 66.1170 | 77.2997 | 79.8171 |
| | GRAE | 81.4912 | 76.7073 | 82.0012 | 82.1278 |
| | HISE | 6.1429 | 4.3462 | 6.1202 | 6.6608 |
| | SFRQ | 6.1512 | 5.9122 | 6.1863 | 6.1416 |
| | Image_ entropy | 7.6658 | 7.4310 | 7.6701 | 7.6757 |

**Table 4. Results of distinguishing distorted vehicle plate numbers with noise ranging from 0.1 to 0.7 for the proposed system**

| New Degraded Image | 0.1 | 0.3 | 0.5 | 0.7 |
|---|---|---|---|---|
| Noise plate 1 | FP | FP | FP | FP |
| Noise plate 2 | TP | FP | FP | FP |
| Noise plate 3 | FP | FP | FP | FP |
| Noise plate 4 | FP | FP | FP | FP |
| Noise plate 5 | TP | TP | TP | FP |

**Table 5. Results of distinguishing distorted vehicle plate numbers with noise ranging from 0.1 to 0.7 for the proposed system**

| New Degraded Image | 0.1 | 0.3 | 0.5 | 0.7 |
|---|---|---|---|---|
| Enhanced plate 1 | TP | FP | FP | FP |
| Enhanced plate 2 | TP | TP | TP | TP |
| Enhanced plate 3 | TP | TP | TP | TP |
| Enhanced plate 4 | TP | FP | FP | FP |
| Enhanced plate 5 | TP | TP | TP | TP |

**Table 6. Shows the recognition rate of deformed vehicle plates**

| | 0.1 | 0.3 | 0.5 | 0.7 |
|---|---|---|---|---|
| **TNPR** | 50% | 33% | 33% | 0 |
| **Proposed NPR** | 100% | 83% | 63% | 66% |

The recognition rate pertains to the precision or success level of accurately identifying or categorizing patterns. It represents the percentage of accurately classified cases among the total number of cases. To calculate the recognition rate, the following formula can be utilized: Recognition rate (RR) = (number of correctly classified instances / total number of instances) * 100 From the final results in Table 10, the proposed NPR system produces peter results compared with the traditional system.

## 5. Conclusion

Despite extensive research efforts, the detection and identification of car license plates pose a significant challenge, particularly when operating under conditions that introduce substantial distortions to the license plate data. The proposed approach demonstrates considerable effectiveness in comparison to existing systems, exhibiting robust performance even with low-resolution and low-contrast images. This achievement is attributed to the strategic application of appropriate filters, yielding satisfactory outcomes. Future investigations should prioritize the development of enhanced artificial intelligence capabilities for the recognition of high-noise, multi-pattern, and multi-plate images. Furthermore, refining the segmentation approach through the utilization of modern image processing tools and techniques holds promise for reducing processing time and elevating recognition rates.

## References


[1] L. Connie, C. Kim On, and A. Patricia, "A Review of Automatic License Plate Recognition System in Mobile Based Platform," *Journal of Telecommunication, Electronic and Computer Engineering*, vol. 10, no. 3-2, pp. 77–82, 2018. [Google Scholar] [Publisher Link]

[2] Sergio Montazzolli Silva, and Claudio Rosito Jung, "Real-Time License Plate Detection and Recognition Using Deep Convolutional Neural Networks," *Journal of Visual Communication and Image Representation*, vol. 71, 2020. [Google Scholar] [Publisher Link]

[3] Roberto A. Lotufo, A.D. Morgan, and A.S. Johnson, "Automatic Number-Plate Recognition," *IEE Colloquium on Image Analysis for Transport Applications*, London, UK, 1990. [Google Scholar] [Publisher Link]

[4] Abhishek Tiwari et al., "Automatic Number Plate and Speed Detection Using YOLO and CNN," *2024 IEEE 9th International Conference for Convergence in Technology*, Pune, India, pp. 1-6, 2024. [CrossRef] [Google Scholar] [Publisher Link]

[5] J.M.S.V. Ravi Kumar, B. Sujatha, and N. Leelavathi, "Automatic Vehicle Number Plate Recognition System Using Machine Learning," *IOP Conference Series: Materials Science and Engineering*: *International Conference on Computer Vision, High Performance Computing, Smart Devices and Networks (CHSN 2020)*, Kakinada, India, vol. 1074, pp. 1-9, 2021. [CrossRef] [Google Scholar] [Publisher Link]

[6] Nur-A-Alam et al., "Intelligent System for Vehicles Number Plate Detection and Recognition Using Convolutional Neural Networks," *Technologies*, vol. 9, no. 1, pp. 1-18, 2021. [CrossRef] [Google Scholar] [Publisher Link]

[7] Tae-Gu Kim et al., "Recognition of Vehicle License Plates Based on Image Processing," *Applied Sciences*, vol. 11, no. 14, pp. 1-12, 2021. [CrossRef] [Google Scholar] [Publisher Link]

[8] Irina Valeryevna Pustokhina et al., "Automatic Vehicle License Plate Recognition Using Optimal K-Means with Convolutional Neural Network for Intelligent Transportation Systems," *IEEE Access*, vol. 8, pp. 92907–92917, 2020. [CrossRef] [Google Scholar] [Publisher Link]

[9] Anatol Maier et al., "Reliability Scoring for the Recognition of Degraded License Plates," *2022 18th IEEE International Conference on Advanced Video and Signal Based Surveillance (AVSS)*, Madrid, Spain, pp. 1-8, 2022. [CrossRef] [Google Scholar] [Publisher Link]

[10] Paula Kaiser et al., "Learning to Decipher License Plates in Severely Degraded Images," *Pattern Recognition: ICPR International Workshops and Challenges, ICPR 2021*, pp. 544–559, 2021. [CrossRef] [Google Scholar] [Publisher Link]

[11] Dilshad Islam, Tanjim Mahmud, and Tanjia Chowdhury, "An Efficient Automated Vehicle License Plate Recognition System under Image Processing," *Indonesian Journal of Electrical Engineering and Computer Science*, vol. 29, no. 2, pp. 1055-1062, 2023. [CrossRef] [Google Scholar] [Publisher Link]

[12] Chun-Cheng Peng, C.-J. Tsai, T.-Y. Chang, J.-Y. Yeh, H. Dai, and M.-H. Tsai, "A Fast and Noise Tolerable Binarization Method for Automatic License Plate Recognition in the Open Environment in Taiwan," *Symmetry*, vol. 12, no. 8, pp. 1-20, 2020. [CrossRef] [Google Scholar] [Publisher Link]

[13] R. Kh. Khamdamov, and H.E. Rakhmanov, "A Character Segmentation Algorithm for Vehicle License Plates," *Cybernetics and Systems Analysis*, vol. 55, pp. 649–654, 2019. [CrossRef] [Google Scholar] [Publisher Link]

[14] Meeras Salman Al-Shemarry, Yan Li, and Shahab Abdulla, "Identifying License Plates in Distorted Vehicle Images: Detecting Distorted Vehicle Licence Plates Using a Novel Preprocessing Methods with Hybrid Feature Descriptors," *IEEE Intelligent Transportation Systems Magazine*, vol. 15, no. 2, pp. 6–25, 2023. [CrossRef] [Google Scholar] [Publisher Link]

[15] Bulent Turan, "A New Approach for SPN removal: Nearest Value Based Mean Filter," *PeerJ Computer Science*, vol. 8, pp. 1-33, 2022. [CrossRef] [Google Scholar] [Publisher Link]

[16] Rafael C. Gonzalez, and Richard E. Woods, *Digital Image Processing*, Addison-Wesley, pp. 1-716, 1992. [Google Scholar] [Publisher Link]

[17] Kai Zhang et al., "Beyond a Gaussian Denoiser: Residual Learning of Deep CNN for Image Denoising," *IEEE Transactions on Image Processing*, vol. 26, no. 7, pp. 3142–3155, 2017. [CrossRef] [Google Scholar] [Publisher Link]

[18] Nada Jasim Habeeb, "Medical Image Denoising with Wiener Filter and High Boost Filtering," *Iraqi Journal of Science*, vol. 64, no. 6, pp. 3123-3135, 2023. [CrossRef] [Google Scholar] [Publisher Link]

[19] Kirti V. Thakur, Omkar H. Damodare, and Ashok M. Sapkal, "Poisson Noise Reducing Bilateral Filter," *Procedia Computer Science*, vol. 79, pp. 861–865, 2016. [CrossRef] [Google Scholar] [Publisher Link]

[20] Umme Sara, Morium Akter, and Mohammad Shorif Uddin, "Image Quality Assessment through FSIM, SSIM, MSE and PSNR—A Comparative Study," *Journal of Computer and Communications*, vol. 7, no. 3, 2019. [CrossRef] [Google Scholar] [Publisher Link]

[21] Ling Meng et al., "A Hybrid Calibration Method for the Binocular Omnidirectional Vision System," *IEEE Sensors Journal*, vol. 22, no. 8, pp. 8059–8070, 2022. [CrossRef] [Google Scholar] [Publisher Link]

[22] Said Pertuz, Domenec Puig, and Miguel Angel Garcia, "Analysis of Focus Measure Operators for Shape-from-focus," *Pattern Recognition*, vol. 46, no. 5, pp. 1415–1432, 2013. [CrossRef] [Google Scholar] [Publisher Link]

[23] M. Subbarao, and J.-K. Tyan, "Selecting the Optimal Focus Measure for Autofocusing and Depth-from-Focus," *IEEE Transactions on Pattern Analysis and Machine Intelligence*, vol. 20, no. 8, pp. 864–870, 1998. [CrossRef] [Google Scholar] [Publisher Link]

[24] Wei Huang, and Zhongiang Jing, "Evaluation of Focus Measures in Multi-Focus Image Fusion," *Pattern Recognition Letters*, vol. 28, no. 4, pp. 493–500, 2007. [CrossRef] [Google Scholar] [Publisher Link]

[25] Saeed Anwar, and Nick Barnes, "Real Image Denoising with Feature Attention," *Proceedings of the IEEE/CVF International Conference on Computer Vision*, pp. 3155-3164, 2019. [Google Scholar] [Publisher Link]

[26] Zbigniew Czapla, "Vehicle Speed Estimation with the Use of Gradient-based Image Conversion into Binary Form," *2017 Signal Processing: Algorithms, Architectures, Arrangements, and Applications (SPA)*, Poznan, Poland, pp. 213-216, 2017. [CrossRef] [Google Scholar] [Publisher Link]

[27] K.A.M. Said, and A.B. Jambek, "Analysis of Image Processing Using Morphological Erosion and Dilation," *Journal of Physics: International Conference on Biomedical Engineering (ICoBE 2021)*, Malaysia, pp. 1-6, 2021. [CrossRef] [Google Scholar] [Publisher Link]

[28] Sunil L. Bangare et al., "Reviewing Otsu's Method for Image Thresholding," *International Journal of Applied Engineering Research*, vol. 10, no. 9, pp. 21777–21783, 2015. [CrossRef] [Google Scholar] [Publisher Link]

[29] Rong Choi Lee, King Chu Hung, and Huan Sheng Wang, "An Automatic Vehicle License Plate Location Based on Sobel Edge Method," *Applied Mechanics and Materials*, vol. 479–480, pp. 911–915, 2013. [CrossRef] [Google Scholar] [Publisher Link]

[30] Ira Kusumadewi et al., "License Number Plate Recognition Using Template Matching and Bounding Box Method," *Journal of Physics: International Conference on Electronics Representation and Algorithm (ICERA 2019)*, Yogyakarta, Indonesia, vol. 1201, pp. 1-9, 2019. [CrossRef] [Google Scholar] [Publisher Link]

[31] Xidong Zhang, "Optimize Vehicle License Plate Recognition System by Image Recognition," *2023 IEEE 5$^{th}$ International Conference on Power, Intelligent Computing and Systems (ICPICS)*, Shenyang, China, pp. 1025-1029, 2023. [CrossRef] [Google Scholar] [Publisher Link]

[32] Dang N.H. Thanh et al., "Impulse Denoising Based on Noise Accumulation and Harmonic Analysis Techniques," *Optik*, vol. 241, 2021. [CrossRef] [Google Scholar] [Publisher Link]

[33] Samet Memiş, and Ugur Erkan, "Different Adaptive Modified Riesz Mean Filter for High-Density Salt-and-Pepper Noise Removal in Grayscale Images," *Avrupa Bilim ve Teknoloji Dergisi*, no. 23, pp. 359–367, 2021. [CrossRef] [Google Scholar] [Publisher Link]